Biogeosciences

Open Access

Solubility of iron and other trace elements in rainwater collected on the Kerguelen Islands (South Indian Ocean)

A. Heimburger, R. Losno, and S. Triquet

Laboratoire Interuniversitaire des Systèmes Atmosphériques, CNRS UMR7583, Université Paris Diderot, Université Paris Est-Créteil, 94010 Créteil Cedex, France

Correspondence to: A. Heimburger (alexie.heimburger@lisa.u-pec.fr)

Abstract. The soluble fraction of aerosols that is deposited on the open ocean is vital for phytoplankton growth. It is believed that a large proportion of this dissolved fraction is bioavailable for marine biota and thus plays an important role in primary production, especially in HNLC oceanic areas where this production is limited by micronutrient supply. There is still much uncertainty surrounding the solubility of atmospheric particles in global biogeochemical cycles and it is not well understood. In this study, we present the solubilities of seven elements (Al, Ce, Fe, La, Mn, Nd, Ti) in rainwater on the Kerguelen Islands, in the middle of the Southern Indian Ocean. The solubilities of elements exhibit high values, generally greater than 70 %, and Ti remains the least soluble element. Because the Southern Indian Ocean is remote from its dust sources, only a fraction of smaller aerosols reaches the Kerguelen Islands after undergoing several cloud and chemical processes during their transport, resulting in a drastic increase in solubility. Finally, we deduced an average soluble iron deposition flux of $27 \pm 6 \, \mu g \, m^{-2} \, d^{-1}$ ($\sim 0.5 \, \mu mol \, m^{-2} \, d^{-1}$) for the studied oceanic area, taking into account a median iron solubility of $82 \% \pm 18 \%$.

1 Introduction

The Southern Ocean is known to be the largest high-nitrate low-chlorophyll (HNLC) oceanic area (de Baar et al., 1995). Such zones are characterized by a lack of micronutrients and trace metals in surface waters, limiting phytoplankton growth (Martin, 1990; Boyd et al., 2000, 2007; Blain et al., 2007). In HNLC areas, primary production is especially limited by iron supply (Boyd et al., 2007) and could be co-limited by other transition metals, such as manganese (Middag et al., 2011), copper (Annett et al., 2008), cobalt (Saito et al., 2002), zinc (Morel et al., 1991) and nickel (Price and Morel, 1991). Atmospheric deposition is recognized as playing an essential role in biogeochemical cycles in remote ocean areas (Duce and Tindale, 1991; Fung et al., 2000; Jickells et al., 2005), even at extremely low levels (Morel and Price, 2003): it brings new external trace metals into surface waters and thus vital bioavailable nutrients for marine biota. It is often assumed that the dissolved forms of trace metals in atmospheric deposition are directly available for phytoplankton because bioavailability is difficult to measure (e. g. Shi et al., 2012). Indeed, bioavailability depends on several factors, which have to be taken into account to determine it, such as the presence of others nutrients in euphotic surface waters, the residence time of deposited atmospheric particles in surface waters, the soluble fraction and the physicochemical speciation of trace metals in seawater (Boyd, 2002; Boyd et al., 2010). Even if phytoplankton only uses a fraction of atmospheric soluble trace metals in its metabolism (Visser et al., 2003), the best proxy so far is taking the soluble fraction of metals as the bioavailable part of these metals for marine biota (Shi et al., 2012). This dissolved fraction expressed as percentage is referred to as "solubility", whose definition depends on the considered science field (e. g. oceanographic and atmospheric sciences) and the usage context. In this paper, we will define solubility in Sect. 3.1. Numerous studies have been carried out on iron solubility and its controlling factors. Soluble iron in soil represents 0.5 % of the total iron (Hand et al., 2004) while it ranges from 0.1–90 % in aerosols, rains and snows, sampled at different places and times (e.g., Losno, 1989; Colin et al., 1990; Zhuang et

Fig. 1a. The Kerguelen Islands in the Southern Indian Ocean.

Fig. 1b. Port-aux-Français on the Kerguelen Islands plus picture of rainwater sampling device on PAF.

al., 1992; Guieu et al., 1997; Edwards and Sedwick, 2001; Kieber et al., 2003; Chen and Siefert, 2004; Baker et al., 2006; Buck et al., 2010b; Theodosi et al., 2010; Witt et al., 2010). Most of the solubility values for atmospheric samples are summarized in Mahowald et al. (2005) and Fan et al. (2006). Variability of iron solubility in the atmosphere is controlled by interactions such as photochemical reactions, cloud processes and organic complexation (e.g., Losno 1989; Zhuang et al., 1992; Kieber et al., 2003; Hand et al., 2004; Chen and Siefert, 2004; Desboeufs et al., 2001, 2005; Paris et al., 2011), as well as mineralogy of dust sources (Journet et al., 2008) and the element's enrichment factor relative to its natural crustal abundance. Baker and Jickells (2006) also suggested that dust iron solubility may instead be controlled by particle size but this hypothesis was contradicted in Buck et al. (2010a) and Paris et al. (2010). All of these factors combined together can explain the wide range of iron solubility values found in the literature. But, it has to be noted here that part of this range is also due to different experimental protocols used by different researchers for investigating the solubility, which hinder our understanding of the factors controlling solubility (e. g. Baker and Croot, 2010; Witt et al., 2010; Shi et al., 2012; Buck and Paytan, 2012; Morton et al., 2013). Other studies have observed that the soluble part of other trace elements is highly variable and heterogeneous too. For example, reported solubility ranges from 0.1–90 % for aluminium and from 10–100 % for manganese (e.g., Jickells et al., 1992; Colin et al., 1990; Losno et al., 1993; Lim et al., 1994; Guieu et al., 1997; Desboeufs et al., 2005; Baker et al., 2006; Buck et al., 2010b; Hsu et al., 2010; Theodosi et al., 2010; Witt et al., 2010).

Compared to the North Hemisphere, atmospheric supply of micronutrients is believed to be small over the Southern Ocean (Fung et al., 2000; Prospero et al., 2002; Jickells et al., 2005; Mahowald et al., 2005) due to its remote distance from
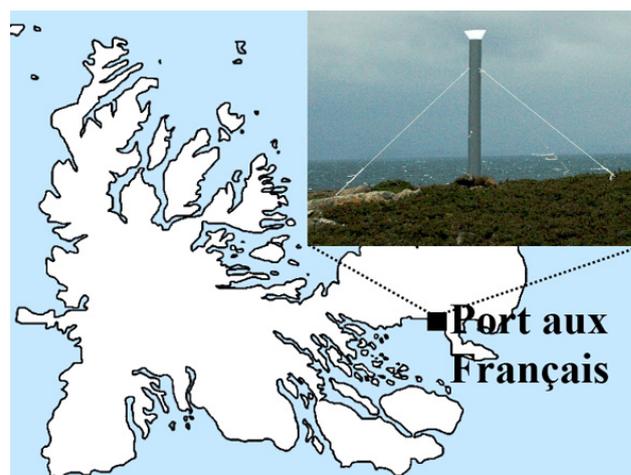
dust sources. In a previous paper, Heimburger et al. (2012a) demonstrated that atmospheric inputs have to be re-evaluated in the Indian part of the Southern Ocean: the authors found that direct measured dust flux is 20 times higher than the previous estimation calculated by Wagener et al. (2008). Therefore, it is highly probable that variation of atmospheric deposition in such an area may strongly influence marine biology and thus carbon sequestration since the Southern Ocean is depicted as the largest potential sink of anthropogenic CO_2 in the global ocean (Sarmiento et al., 1998; Caldeira and Duffy, 2000; Schlitzer, 2000). In this paper, we present measurements of soluble and insoluble composition for crustal elements, including iron, in rainwater samples collected on the Kerguelen Islands in the Southern Indian Ocean. To our knowledge up to now such measurements have never been taken over this oceanic region.

2 Materials and methods

2.1 Sampling site

The studied area was located on the Kerguelen Archipelago (48°35′–49°54′ S; 68°43′–70°35′ E), in the Southern Indian Ocean, approximately 3800 km south-east of South Africa and 2000 km from the Antarctic coast (Fig 1a). Rain sampling was carried out during four summer campaigns, one under the program KEFREN ("Kerguelen : Erosion and Fallout of tRace Elements and Nitrogen") and three under the FLA-TOCOA one ("Flux Atmosphérique d'Origine Continentale sur l'Océan Austral"). Both programs were supported by IPEV ("Institut polaire français Paul Emile Victor"). A total of 14 single rain events were collected; they are divided as follows: (i) two rains were collected from 30 January to 13 February 2005 (named P1/2_05 and P5_05), (ii) three rains from 3–11 December 2008 (P3_08, P5_08, P6_08),

Fig. 2a. Rainwater sampling device on the top of its PVC tube.

Fig. 2b. Drawing of the sampling device, the sampling funnel is cut here.

(iii) four rains from 5 December 2009 to 4 January 2010 (P2_09, P3_09, P6_09, P7_09) and (iv) five rains from 24 November to 11 December 2010 (from P1_10 to P5_10). The sampling site ($49°21'10.3''$ S, $70°12'58.3''$ E) was installed near the chapel Notre Dame des Vents, north-west of the only permanently-occupied base of the archipelago Port-aux-Français (PAF) (Fig. 1b).

2.2 Materials

Rains were sampled using a collector placed on top of a 100 mm diameter and 2 m-high, vertically erected PVC pipe (Fig. 2a). This collector is made from a 24 cm diameter low-density polyethylene (PE) funnel attached to an online filtration device (Fig. 2b). The filtration device is composed of several parts: a machined high-density PE cable fitting holds the bottom end of the funnel and supports a Teflon® filter holder equipped with a clipped Nuclepore® polycarbonate membrane (PC) filter (porosity : 0.2 µm, diameter : 47 mm) on a PC supporting grid. The filter holder is placed on the top of a 30 cm-high closed section of tubing that is fitted to a 500 mL polypropylene (PP) bottle. A small Teflon® pipe lets filtered water flow freely into the bottle. The insoluble fraction of rainwater remains on the surface of the PC filter while the soluble fraction flows by gravity into the PP bottle (Nalgene®). The only pieces of equipment that touch the rainwater are the funnel, the Teflon® filter holder, the PC filters, the PC filter supporting grid and the PP bottles (Fig. 2b).

All the sampling materials were thoroughly washed in the laboratory before the campaigns. The 500 mL PP bottles and Teflon® parts underwent the same washing protocol as described in Heimburger et al. (2012a) for total deposition devices. All of the other materials were: (i) washed using ordinary dish detergent in an ISO 8-controlled laboratory room, (ii) soaked from two days to one week in a bath of 2 % Decon® detergent diluted with reverse-osmosed water
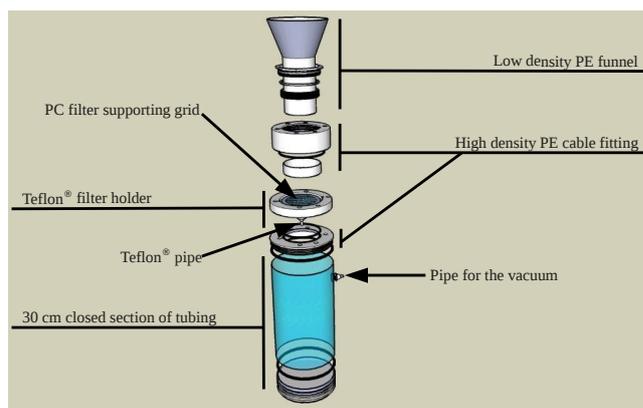
(purified water) and (iii) soaked from two to three weeks in 2 % v/v Normapur® analytic grade hydrochloric acid. Extensive rinsing was performed between each step with reverse-osmosed water. Materials were then transferred to an ISO 5 cleanroom and: (iv) rinsed in Elga™ Purelab ultra® pure water and (v) soaked in a high-purity hydrochloric acid solution (2 % Merk™ Suprapur®), except for the funnels, which were too large for our soaking baths. In an ISO 1 laminar flow bench, these materials were finally: (vi) rinsed once (three times for the funnels) with 2 % high purity hydrochloric acid solution, (vii) five times with ultra pure water and (viii) left until dry (two to four hours). Once all the materials had been washed and dried, the funnels were mounted on their high-density PE cable fittings under the ISO 1 laminar flow bench and the last three steps of the washing protocol were repeated. They were then individually placed in bags that had been washed in the same way as the materials, and were stored until being used only once in the field. The Nuclepore® PC filters (0.2 µm porosity, diameter : 47 mm) were (i) washed in a bath of 2 % v/v Romil-UpA™ HCl for almost 2 h under the ISO 1 laminar flow bench, then (ii) rinsed with ultra pure water, (iii) clipped with special rings (FilClip®), previously washed by the protocol for materials described above, and (iv) stored individually in washed polystyrene Petri dishes until use.

2.3 Rain sampling

A clean hood (AirC2, ISO 2 quality), which provided an ultra-clean work zone, was installed inside a dedicated clean area (ISO 6-ISO 7 quality) in the PAF scientific building (see Heimburger et al. (2012a) for more details). It allowed us to prepare rain devices before sampling: (i) a clipped filter was placed in the Teflon® filter holder, (ii) a 500 mL PP bottle without its cork was introduced into the 30 cm-high closed tubing (the cork was stored in a clean box intended for this purpose), and (iii) a funnel with its cable fitting + Teflon® filter holder were screwed on to the top of the closed tubing.

The plastic bag protecting the funnel's aperture had to be kept in place; a crack was made at the level of the cable fitting.

The sampling started at the beginning of a rain event. A prepared rain device was placed on the top of the PVC pipe; the plastic bag protecting the funnel was removed and conserved. Once the rain event had finished, the funnel was covered by its plastic bag and the device was brought into the clean hood in the scientific building. A vacuum was applied to the section of tubing to help the last rain drops to pass through the filter. The funnel was then removed and no longer used (a new one was used for each sampling). The clipped filter was stored in a clean Petri dish and the 500 mL bottle was weighed. Finally, less than half on hour after the collection of the sample, part of the soluble fraction of rain was stored in a 60 mL Teflon® bottle. Teflon® bottles have undergone the same washing protocol as the 500 mL bottles. They contained enough Romil-UpA™ HNO$_3$ to give a 1 % concentration of acid when filled with the collected rain; the acid solution was used to prevent adsorption of trace metals into the Teflon® bottle walls during the storage of samples (between six months and two years) before trace metal analyses back in the laboratory. During the 2008 campaign, the pH of samples was immediately measured after sampling: it is equal to 5.4 ± 0.2 (mean $\pm \sigma$, $\sigma =$ standard deviation) for all the samples. The Teflon® filter holder was then rinsed once with 2 % Merk™ Suprapur® hydrochloric acid solution, five times with ultra pure water and allowed to dry in the clean hood before being used for the next sampling. Four laboratory blanks and eight field blanks were performed by simulating a rain event with Elga™ Purelab ultra® pure water in an ISO 5 cleanroom and in the field, respectively.

2.4 Sample preparation and analyses

Back in the laboratory and just before analyses, the soluble fractions of rains (stored in 60 mL 1 % HNO$_3$ acidified Teflon® bottles) were transferred into PP 15 mL sample vials that had been thoroughly washed (see Heimburger et al. (2012a) for details of the washing protocol). The contents of vials were analysed using high-resolution inductively coupled plasma mass spectrometry (HR-ICP-MS, Thermo Fisher Scientific™ Element 2), which was installed in an ISO 5 cleanroom and calibrated by diluted acidified multi-element external standards. The sample introduction system was protected by an ISO 1 box.

The contours of the clipped filters, which contained the insoluble fractions of rains, were cut using a new, clean, stainless steel scalpel blade. The filters of rain samples, laboratory blanks and field blanks were then digested using 4 mL of a HNO$_3$ / H$_2$O / HF solution (proportion: 3/1/0.5 of pure Romil-UpA™HNO$_3$/ultra pure water/Merk™ Ultrapur® HF) during 14 h in an air oven at 130 °C in closed Savillex™ PFA digestion vessels. Vessels had undergone the same washing protocol as described in Heimburger et al. (2012a) followed by a trial digestion. These vessels were then rinsed and filled with 2 % Romil-UpA™ HCl until being used. At the end of digestion, the HF was completely evaporated on a heater plate. Overall, 5 mL of 1 % Romil-UpA™ HNO$_3$ plus 0.5 mL of Romil-UpA™ H$_2$O$_2$ were then added and left on the plate for 30 min. Finally, the content of each vessel was transferred into a 60 mL PP bottle (same washing protocol as for the bottles containing rain samples) with the 1 % Romil-UpA™ HNO$_3$ solution used to rinse the vessel walls. These samples were then analysed by HR-ICP-MS as well. Seven blank Nuclepore® PC filters underwent the digestion protocol in order to estimate possible contamination from the filters and the digestion experiments. A total of 6 mg of BE-N (Basalt from SARM laboratory, France) and 8.6 mg of SDC-1 (Mica Schist from USGS, USA) geostandards, crushed prior to use, also underwent this protocol in order to estimate the yield and accuracy of our digestion method.

Analytical blanks ($n = 7$) were carried out using 1 % v/v Romil-UpA™ HNO$_3$ in order to determine the analytical detection limits (DL) of the HR-ICP-MS method. The accuracy (expressed as recovery rate: RR % = mean of measured standard concentrations/certified or published values) and reproducibility (expressed as relative standard deviation: RSD % $= \sigma$/mean) of measurements were checked using the certified reference material (CRM) SLRS-5 (Heimburger et al., 2012b) commonly used to control trace metals analysis. This CRM was diluted ten times using 1 % v/v Romil-UpA™ ultra-pure nitric acid in ultra-pure water in order to find more similar concentrations between the SLRS-5 and the ones found in samples, allowing calculation of significant RR % and RSD % (Feinberg, 2009). Table 1 presents DL, RSD % and RR % for a set of analysed elements, for which results were validated (see Sect. 3.1) and so discussed afterwards. All the measured concentrations including blanks were above DL: they are three times higher than DL in samples, except for Nd for the soluble fraction. Reproducibility of SLRS-5 measurements is under or equal to 10 % for all the elements; accuracy is between 94 and 109 %. Measured concentrations in BE-N and SDC-1 geostandards are fairly consistent with the certified ones: RR % are generally equal to 100 % $\pm$ 30 % .

3 Results and discussion

3.1 Solubility uncertainties

The solubility in rainwater is expressed as follows:

$$S_X \% = \frac{[X]_{\text{soluble}}}{[X]_{\text{total}}}, \tag{1}$$

where S_X % is the solubility of an element X, $[X]_{\text{soluble}}$ is the soluble concentration of X, $[X]_{\text{insoluble}}$ is the insoluble concentration of X and $[X]_{\text{total}}$ is the sum of $[X]_{\text{soluble}}$ and $[X]_{\text{insoluble}}$. The soluble fraction is defined here as the amount of metals in rainwater which passes through the

Table 1. Detection limits, accuracy and reproducibility of SLRS-5 measurements, estimated recovery rate of BE-N and SDC-1.

Element	m/z (res.)	DL (ng L^{-1})	SLRS-5			BE-N	SDC-1
			measured values $\pm \sigma$ (μg L^{-1})	RSD %	RR %	RR %	RR %
Al	27 (m)	26.4	51 ± 3	6 %	102 %	112 %	74 %
Ce	140 (l)	0.036	0.257 ± 0.014	5 %	109 %	121 %	
Fe	56 (m)	5.2	93 ± 5	5 %	102 %	129 %	105 %
La	139 (l)	0.039	0.199 ± 0.011	5 %	101 %	111 %	
Mn	55 (m)	0.62	4.5 ± 0.2	5 %	104 %	143 %	111 %
Nd	146 (l)	0.11	0.183 ± 0.008	4 %	99 %	112 %	
Ti	47 (m)	1.7	2.1 ± 0.2	10 %	94 %	151 %	109 %

m/z = mass of the considered isotope; res. = resolution; h = high resolution ($> 10\,000$), m = medium resolution (≈ 4000), l = low resolution (≈ 300); DL = detection limit; RSD % = reproducibility, RR % = recovery rate.
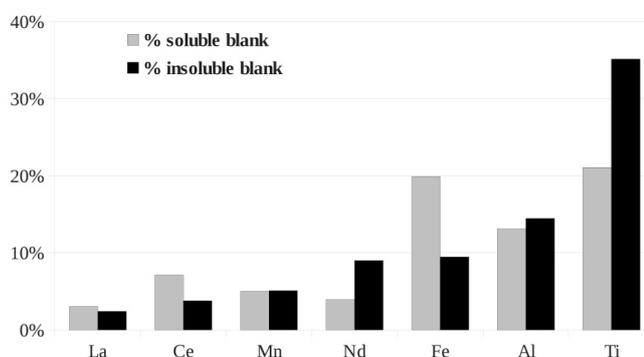
Fig. 3. Ratio of the median quantities in blanks (all the blanks pooled together) relative to both median soluble (grey) and median insoluble (black) quantities in rainwater samples for all the measured elements.

0,2 μm PC membrane filter. The insoluble one is defined as the amount which stays on the PC filter. If we assume that rainwater is aerosol particles trapped in water drops, solubility is then defined as the fraction of metals that is dissolved in rainwater (i. e. the metal content in the filtrated rain divided by the total metal content in rain) (e.g. Lim et al., 1994; Buck et al., 2010b). This solubility is related to the *fractional solubility* defined by Baker and Croot (2010) for laboratory experiments on aerosol dissolution. Filtration of rainwater during the sampling provides a direct measurement of natural solubility.

To determine $[X]_{\text{soluble}}$ and $[X]_{\text{insoluble}}$, we took into account the contamination observed in the different blanks performed (laboratory blanks, field blanks, blank filters; see Sect. 2.) for both soluble and insoluble fractions, respectively. This contamination is caused by elements remaining in sampling devices, including filters and the walls of equipment in contact with samples. For a given element X, we computed its quantities (Q_i) in each blank by multiplying measured blank concentrations by blank volumes. For the elements presented in this paper, these quantities are found

to be similar for both laboratory and field blanks; the quantities in filter blanks are also equivalent to the ones in laboratory and field-insoluble blanks. Therefore, all the blanks were pooled together for both fractions, respectively, in order to extract a global blank defined as the median quantity of all the blank quantities. Figure 3 represents ratios of this median quantity in blanks relative to the one in rainwater, for all the analysed elements in the soluble and insoluble fractions, respectively. Expressed as a percentage, these ratios are under 10 % for Ce, La, Mn and Nd for both fractions, under 20 % for Al and Fe for both fractions, and reach 35 % for Ti for the insoluble fraction only. It has to be noted here that other elements (Co, Cr, Cu, Ni, V, Pb, Zn) were also analysed in rainwater but their ratio values (median quantity in blanks relative to the one in rainwater) were higher than 40 % for the both soluble and insoluble fractions, and even equal to 100 % for Ni and Cu. Thanks to all the blanks we performed, this contamination was identified as coming from PC filters. Despite careful washing of these filters, filter blanks exhibit high quantities of Co, Cu, Cr, Ni, V, Pb and Zn compared to the median quantities found in rain samples for these elements after blank corrections. It leads to a contamination of the soluble fraction of laboratory and field blanks, for which no other significant contamination were observed.

For the validated elements (Al, Ce, Fe, La, Mn, Nd, Ti), the median quantity in blanks was subtracted from the ones found in rain samples for each element. $[X]_{\text{soluble}}$ and $[X]_{\text{insoluble}}$ are consequently given by the following formulas:

$$[X]_{\text{soluble}} = \frac{[X]_{\text{analytical}} V_{\text{rain}} - \text{median}(Q_i)}{V_{\text{rain}}} \quad (2)$$

$$[X]_{\text{insoluble}} = \frac{[X]_{\text{analytical}} V_{\text{insoluble}} - \text{median}(Q_i)}{V_{\text{rain}}}, \quad (3)$$

where $[X]_{\text{analytical}}$ represents measured concentrations, V_{rain} the volumes of collected rainwater, and $V_{\text{insoluble}}$ the dilution
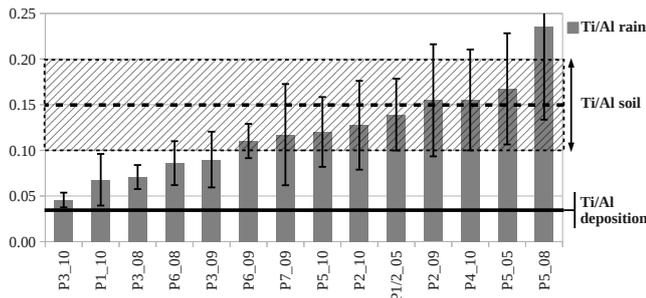
Fig. 4. Ti / Al ratios in rainwater samples (grey histogram), in soil samples (dotted black line + hatched rectangle for uncertainties; Heimburger et al., 2012a) and in deposition samples (black line; Heimburger et al., 2012a). Ti / Al in P3_10, P1_10, P3_08, P6_08 and P3_09 exhibit values not compatible with the range of Ti / Al found in soil collected on the Kerguelen Islands; these five rains were then considered as not significantly influenced by local soil contamination and so representative of long-range transport particles.

volumes of the digested insoluble fraction. Uncertainties associated with $[X]_{\text{analytical}}$ ($\sigma([X]_{\text{analytical}})$) are computed using standard deviations and the mathematical approach of exact differential (Feinberg, 2009). Because the quantities of all the blanks are not normally distributed, we used robust statistics for a better estimation of the blank distribution range (Feinberg, 2009):

$$\sigma\left([X]_{\text{analytical}}\right) = \sqrt{\text{DL}^2 + \left([X]_{\text{analytical}}\,\text{RSD\%}\right)^2 + \left([X]_{\text{analytical}}\,(1-\text{RR\%})\right)^2} \quad (4)$$

where (1 - RR %) is the accuracy error from SLRS-5 measurements. Standard deviations of $[X]_{\text{soluble}}$ and $[X]_{\text{insoluble}}$ are then computed as follows:

$$\sigma\left([X]_{\text{soluble}}\right) = \frac{\sqrt{\left(\sigma[X]_{\text{analytical}}\,V_{\text{rain}}\right)^2 + (1.483\text{MAD})^2}}{V_{\text{rain}}} \quad (5)$$

$$\sigma\left([X]_{\text{insoluble}}\right) = \frac{\sqrt{\left(\sigma[X]_{\text{analytical}}\,V_{\text{insoluble}}\right)^2 + (1.483\text{MAD})^2}}{V_{\text{rain}}} \quad (6)$$

with median absolute deviation (MAD) = median($|Q_i - \text{median}(Q_i)|$) representing the dispersion of blank distribution. Finally, solubility uncertainties are given by the Eq. (7):

$$\Delta S_X\% = k\,S_X\%\,\frac{\sqrt{\left(\frac{\sigma[X]_{\text{soluble}}}{[X]_{\text{soluble}}}\right)^2 + \left(\frac{\sigma[X]_{\text{insoluble}}}{[X]_{\text{insoluble}}}\right)^2}}{1 + \frac{[X]_{\text{soluble}}}{[X]_{\text{insoluble}}}}, \quad (7)$$

with the coverage factor of $k = 2$ (Feinberg, 2009), which allows us to obtain an expanded uncertainty representing a confidence level of 95 %, i.e. this expanded uncertainty includes 95 % of possible solubility values.

3.2 Local contamination issues

Rain samples may be contaminated by local soil emission due to human activities on PAF occurring not far enough from the sampling site: soil portions are occasionally moved because of track maintenance generating exposed surfaces that produce local emission spots. Heimburger et al. (2012a) demonstrated that Ti / Al ratio is a suitable tracer for such contamination: the authors reported that these ratios are equal to 0.15 ± 0.05 (mean $\pm \sigma$) and 0.04 ± 0.01 in soil and atmospheric deposition samples, respectively. Consequently, the $[\text{Ti}]_{\text{total}}/[\text{Al}]_{\text{total}}$ ratio was computed for each rain sample (Fig. 4). Uncertainty on this ratio was computed by the following formulas:

$$\sigma\left(\frac{[\text{Ti}]_{\text{total}}}{[\text{Al}]_{\text{total}}}\right) = (\text{Ti}/\text{Al})\sqrt{\left(\frac{\sigma\,[\text{Ti}]_{\text{total}}}{[\text{Ti}]_{\text{total}}}\right)^2 + \left(\frac{\sigma\,[\text{Al}]_{\text{total}}}{[\text{Al}]_{\text{total}}}\right)^2} \quad (8)$$

with

$$\sigma\left([X]_{\text{total}}\right) = \sqrt{\sigma\,[X]_{\text{insoluble}}^2 + \sigma\,[X]_{\text{soluble}}^2}. \quad (9)$$

Rains from P6_09 to P5_08 in Fig. 4 present Ti / Al ratios consistent with the one found in Kerguelen's soil, which is not compatible with pure long-range transported particles, and so they were not discussed afterwards. Rain P3_10 exhibits a Ti / Al ratio incompatible with local soil contamination and in the range found in deposition samples (Heimburger et al., 2012a). Four rains (P1_10, P3_08, P6_08, P3_09) have a Ti / Al ratio between the ones in soils and in deposition. If we take into account standard deviation calculated with the Eq. 8 and Eq. 9, a local soil contamination is less probable for P1_10 and P3_08 than for P6_08 and P3_09, for which a small recovery of ranges of both soils and samples is observed. Nevertheless no strong discriminating criterion was found for these four rains and so, they will be included with rain P3_10 in the following discussion (insoluble and soluble concentrations of these five selected rains are available in supplementary reading).

To insure that no other local contamination from anthropogenic activities were taking place on PAF, we used Global Data Assimilation System (GDAS)-reanalysed archives (Draxler and Rolph, 2012; Rolph, 2012) to observe wind direction during the respective sampling times of the five kept rains. The base PAF is located east of the sampling site. For the five non-contaminated rains, winds came from opposite sectors of PAF, excluding wind-transported contamination from the base (see sampling conditions on Table 2a). Sampling conditions for contaminated rains are displayed on Table 2b.

3.3 Rain event fluxes

Deposition fluxes generated by single rain events were computed by dividing the quantities found in each validated rain sample by the surface of the funnel aperture ($0.045\,\text{m}^2$). In

Table 2a. Sampling conditions for the non-contaminated rain events. The funnel collecting surface is $0.045 \, \mathrm{m}^2$.

Sample name	Sampling period	Collected volume	Wind direction
P3_08	7/12/2008 from 8:30 to 11:55	0.320 L	W-SW
P6_08	from 10/12/2008 (22:30) to 11/12/2008 (19:00)	0.101 L	W-NW
P3_09	11/12/2009 from 8:05 to 17:30	0.029 L	W-SW
P1_10	from 24/11/2010 (19:00) to 25/11/2010 (9:00)	0.536 L	W-NW
P3_10	30/11/2010 from 15:50 to 22:30	0.453 L	N-NW

Table 2b. Sampling conditions for the possible contaminated rain events.

Sample name	Sampling period	Collected volume	Wind direction
P1/2_05	30/01/2005 from 5:40 to 8:30	0.460 L	NE
P5_05	from 12/02/2005 (17:00) to 13/02/2005 (3:36)	0.550 L	N-NW
P5_08	from 9/12/2008 (20:00) to 10/12/2008 (12:00)	0.317 L	NE to NW
P2_09	7/12/2009 from 10:15 to 14:20	0.085 L	NW
P6_09	28/12/2009 from 11:45 to 17:00	0.538 L	N to NW
P7_09	from 3/01/2010 (18:00) to 4/01/2010 (6:00)	0.333 L	N to W
P2_10	from 26/11/2010 (10:45) to 28/11/2010 (11:00)	0.041 L	N-NW to W
P4_10	from 30/11/2010 (22:30) to 01/12/2010 (7:00)	0.210 L	NW to SW
P5_10	from 6/12/2010 (7:45) to 09/12/2010 (8:30)	0.538 L	NE to NW

Heimburger et al. (2013), the authors found that atmospheric total deposition fluxes for the oceanic area of the Kerguelen and Crozet Islands, averaged over 2009–2010, are equal to $53 \pm 2 \, \mu\mathrm{g} \, \mathrm{m}^{-2} \, \mathrm{d}^{-1}$ and $33 \pm 1 \, \mu\mathrm{g} \, \mathrm{m}^{-2} \, \mathrm{d}^{-1}$ for Al and Fe, respectively. Here, we found averaged rain fluxes (wet fluxes) equal to (mean $\pm \sigma$) $24 \pm 18 \, \mu\mathrm{g} \, \mathrm{m}^{-2}$ per rain events for Al and $14 \pm 10 \, \mu\mathrm{g} \, \mathrm{m}^{-2}$ per rain events for Fe (Table 3a). Because dust deposition is controlled by wet deposition on the Kerguelen Islands (Heimburger et al., 2012a), we can neglect the dry deposition flux and thus we can assimilate total deposition flux to the wet deposition one (rainwater events). Taking into account meteorological data that we recorded 8 km from PAF, rain events occur from once a day to every two days, and so with a frequency of 0.5 to 1 per day. Applying this frequency on deposition flux values from Heimburger et al. (2013), the averaged deposition flux on the Kerguelen Islands is 51–$110 \, \mu\mathrm{g} \, \mathrm{m}^{-2}$ per rain event for Al and 32–$68 \, \mu\mathrm{g} \, \mathrm{m}^{-2}$ per rain event for Fe. These flux values are higher than the ones found in rainwater but they have the same order of magnitude. We can then conclude that rain samples studied in this paper are not unusual events.

Table 3b shows deposition fluxes calculated from contaminated rainwater samples. Their median is on average two times higher than the ones calculated from non-contaminated samples for Al, Mn, Fe and Ti and one and a half higher for La, Nd and Ce. This observation is consistent with the hypothesis of a local contamination, which added material in rain samples.

3.4 Solubility

Before this study, no observed solubility values in rainwater were available in the literature for the oceanic area of the Kerguelen Islands. Our values can help to better quantify and model (chemistry and transport) the part of atmospheric iron, which can be bioavailable for phytoplankton in the Southern Indian Ocean. Solubilities in rains are reported in Table 4: they are higher than 70 % for all the elements (Al, Ce, Fe, La, Mn, Nd, Ti) for the five considered rain, except for Ti (33 % $\pm$ 29 % and 46 % $\pm$ 29 %) and Fe (57 % $\pm$ 19 % and 51 % $\pm$ 22 %) in P1_10 and P3_09, respectively (Table 4a). The rare earth elements (La, Ce and Nd) also exhibit high-solubility values ranging from 68 % to 98 % (Table 4a). In contrast, solubilities measured for the rejected rain samples generally show much lower values (Table 4b), with a median of 16 % for Ti, 9 % for Fe and 19 % for Al. This supports the hypothesis of a contamination by insoluble particles from local soils.

High solubilities were already observed for some of these elements in the literature. Siefert et al. (1999) wrote that "labile Fe" solubility in the fine dust fraction is more than 80 % in aerosols collected onboard, while Edwards and Sedwick (2001) reported an Fe solubility ranging from 9 to 89 % in snow samples collected in Antarctica and Baker and Croot (2010) modelled an Fe solubility between 0.2 and 100 % over the Southern Indian Ocean. Witt et al. (2010) found that Al solubility can reach 91 % $\pm$ 66 % when the soluble fraction of aerosols collected in the North Indian Ocean was extracted with a pH 1 solution. Mn solubility can reach more than 90 % in oceanic areas (Baker et al., 2006) and is

Table 3a. Rain event fluxes (μg m^{-2}) $\pm$ uncertainties, deduced from measurements of the non-contaminated samples.

	P3_08	P6_08	P3_09	P1_10	P3_10
Al	32 ± 5	11 ± 3	12 ± 3	12 ± 3	52 ± 7
Ce	0.048 ± 0.010	0.021 ± 0.005	0.021 ± 0.004	0.024 ± 0.005	0.11 ± 0.02
Fe	13 ± 3	8.3 ± 3.2	7.5 ± 3.4	8.5 ± 3.4	31 ± 4
La	0.025 ± 0.003	0.011 ± 0.001	0.0090 ± 0.0009	0.011 ± 0.001	0.041 ± 0.004
Mn	0.34 ± 0.06	0.23 ± 0.05	0.21 ± 0.06	0.82 ± 0.11	1.3 ± 0.2
Nd	0.018 ± 0.002	0.0079 ± 0.0008	0.0075 ± 0.0008	0.0069 ± 0.0015	0.043 ± 0.004
Ti	2.2 ± 0.8	0.98 ± 0.49	1.1 ± 0.7	0.82 ± 0.65	2.4 ± 0.8

Uncertainties are computed by propagating standard deviations of Eqs. (5) and (6).

Table 3b. Rain event fluxes (μg m^{-2}) $\pm$ uncertainties, deduced from measurements of samples identified as contaminated by local emission.

	P1/2_05	P5_05	P5_08	P2_09	P6_09
Al	19 ± 4	118 ± 40	6.6 ± 3.3	21 ± 8	23 ± 4
Ce	0.025 ± 0.005	0.16 ± 0.05	0.0093 ± 0.0027	0.027 ± 0.009	0.039 ± 0.008
Fe	30 ± 5	107 ± 36	6.6 ± 3.8	$-$	15 ± 4
La	0.0092 ± 0.0012	0.064 ± 0.011	0.0038 ± 0.0006	0.0095 ± 0.0017	0.015 ± 0.002
Mn	1.5 ± 0.2	2.2 ± 0.9	0.20 ± 0.07	0.38 ± 0.17	0.65 ± 0.09
Nd	0.0084 ± 0.0015	0.057 ± 0.010	0.0032 ± 0.0010	0.0079 ± 0.0015	0.015 ± 0.002
Ti	2.6 ± 1.4	20 ± 13	1.5 ± 1.1	3.2 ± 2.3	2.5 ± 0.7

	P7_09	P2_10	P4_10	P5_10
Al	7.4 ± 3.3	24 ± 8	49 ± 15	29 ± 6
Ce	0.015 ± 0.004	0.034 ± 0.010	0.076 ± 0.021	0.061 ± 0.011
Fe	5.5 ± 3.7	18 ± 7	41 ± 14	22 ± 6
La	0.0033 ± 0.0006	0.016 ± 0.002	0.029 ± 0.004	0.028 ± 0.003
Mn	0.22 ± 0.06	0.70 ± 0.21	1.1 ± 0.4	1.7 ± 0.2
Nd	0.0023 ± 0.0010	0.013 ± 0.002	0.027 ± 0.004	0.024 ± 0.002
Ti	0.87 ± 0.72	3.1 ± 2.1	7.6 ± 4.9	3.5 ± 2.1

known to be highly variable (Losno, 1989; Desboeufs et al., 2005; Buck et al., 2010b). Nonetheless, Ti solubility generally exhibits a lower value ($< 15\,\%$) (Buck et al., 2010b; Hsu et al., 2010) than the ones found on the Kerguelen Islands (median $= 76\,\% \pm 13\,\%$) although Ti remains the least soluble element in our samples. We did not find any previously published solubility values for La, Ce or Nd. High solubility of Ti informs us that dissolution processes in the atmosphere are very efficient and probably destroy all the solid phases forming original aerosols, including the ones containing REE.

Several studies demonstrate that aerosol solubility increases during particle transport, especially due to cloud processes (Zhuang et al., 1992; Gieray et al., 1997; Desboeufs et al., 2001). It is believed that during their transport in the atmosphere aerosols typically undergo around 10 condensation/evaporation cloud cycles (Pruppacher and Jaenicke, 1995). In clouds, trace gases, such as HNO$_3$, SO$_2$ and NH$_3$, are present and modify the pH of cloud droplets, which can increase the soluble fraction of mineral particles. Organic molecules can also increase solubility, e.g. oxalate complex-

ation promoting iron solubility (Paris et al., 2011), as well as photochemistry processes, as reviewed in Shi et al. (2012). Moreover, the average size of mineral aerosols decreases with distance from dust sources, as a result of higher deposition rates for larger particles (Duce et al., 1991). When mineral aerosol size becomes smaller, a greater proportion of their volume is exposed to surface processes (Baker and Jickells, 2006) and is therefore available for dissolution. Ito (2012) supports the hypothesis that smaller dust particles yield increased iron solubility relative to larger particles as a result of acid mobilization in smaller particles. As a consequence, the smaller the aerosols are and the further they are from their source area, the more soluble they are (Baker and Jickells, 2006). Taking into account both of these hypotheses, we can explain the high solubilities observed on the Kerguelen Islands by long-range transport from dust sources, which have been identified as South America, South Africa and/or Australia (Prospero et al., 2002; Mahowald et al., 2007; Bhattachan et al., 2012). Indeed, Wagener et al. (2008) and Heimburger et al. (2012a) noted that particles observed on the Kerguelen Islands at sea- or ground level exhibit 2 μm

Table 4a. Solubility (%) in rainwater for the five non-contaminated samples.

	P3_08	P6_08	P3_09	P1_10	P3_10	Median
Al	92 % ± 4 %	95 % ± 6 %	67 % ± 12 %	70 % ± 12 %	96 % ± 2 %	92 %
Ce	94 % ± 2 %	92 % ± 4 %	68 % ± 9 %	84 % ± 6 %	96 % ± 1 %	92 %
Fe	82 % ± 8 %	85 % ± 9 %	51 % ± 22 %	57 % ± 19 %	91 % ± 4 %	82 %
La	95 % ± 1 %	96 % ± 2 %	70 % ± 5 %	83 % ± 4 %	96 % ± 1 %	95 %
Mn	88 % ± 6 %	89 % ± 7 %	66 % ± 14 %	89 % ± 6 %	94 % ± 3 %	89 %
Nd	95 % ± 2 %	98 % ± 3 %	70 % ± 5 %	79 % ± 6 %	96 % ± 1 %	95 %
Ti	76 % ± 21 %	83 % ± 35 %	46 % ± 29 %	33 % ± 29 %	79 % ± 20 %	76 %

Absolute uncertainties (±) are computed using Eq. 7 for each rain sample.

Table 4b. Solubility (%) in possible contaminated rainwater samples.

	P1/2_05	P5_05	P5_08	P2_09	P6_09
Al	59 % ± 11 %	3 % ± 2 %	19 % ± 31 %	5 % ± 11 %	91 % ± 5 %
Ce	51 % ± 11 %	6 % ± 3 %	38 % ± 14 %	3 % ± 5 %	90 % ± 4 %
Fe	70 % ± 9 %	6 % ± 3 %	9 % ± 42 %	–	83 % ± 7 %
La	47 % ± 6 %	7 % ± 2 %	40 % ± 8 %	5 % ± 3 %	89 % ± 2 %
Mn	80 % ± 9 %	21 % ± 9 %	49 % ± 17 %	20 % ± 11 %	94 % ± 4 %
Nd	49 % ± 9 %	5 % ± 3 %	39 % ± 17 %	1 % ± 5 %	90 % ± 3 %
Ti	35 % ± 19 %	1 % ± 1 %	17 % ± 15 %	2 % ± 5 %	89 % ± 17 %

	P7_09	P2_10	P4_10	P5_10	Median
Al	30 % ± 25 %	18 % ± 10 %	14 % ± 6 %	59 % ± 10 %	19 %
Ce	27 % ± 11 %	18 % ± 7 %	21 % ± 7 %	72 % ± 8 %	27 %
Fe	3 % ± 53 %	8 % ± 16 %	7 % ± 7 %	38 % ± 12 %	9 %
La	31 % ± 9 %	23 % ± 4 %	20 % ± 4 %	79 % ± 4 %	31 %
Mn	64 % ± 14 %	45 % ± 14 %	32 % ± 12 %	84 % ± 7 %	49 %
Nd	19 % ± 33 %	21 % ± 4 %	21 % ± 4 %	77 % ± 4 %	21 %
Ti	21 % ± 23 %	4 % ± 6 %	5 % ± 4 %	16 % ± 11 %	16 %

median diameters, suggesting that only the fine dust fraction, which is believed to be more soluble than the larger dust fraction, reaches the Kerguelen Islands. In addition, air mass back trajectories computed from a Hybrid Single Particle Lagrangian Integrated trajectory from the NOAA Air Resource Laboratory (HYSPLIT) model (Draxler and Rolph, 2012; Rolph, 2012) with re-analysed archived meteorological data (GDAS) show that air masses travelled for at least five days over the ocean before arriving at our sampling location during the five-rain collection period. These air masses did not pass over continents and so did not gain new, less soluble continental aerosols. As a consequence, continental aerosols coming to the Kerguelen Islands underwent several cloud processes during their long-range transport in the atmosphere and over the ocean, which probably dramatically increased their solubilities.

4 Conclusions

Out of a total of 14 single rain events collected on the Kerguelen Islands, five samples considered free of local contam-

ination were validated and are representative of long-range transported particles deposited by rain events. Soluble and insoluble fractions of rainwater were immediately separated during sampling, allowing chemical evolution of some elements, such as Fe, to be kept to a minimum. We found very high solubilities ($> 70\,\%$) for all the analysed elements, even the rare earth elements, for which these are the first solubility values to be measured in an oceanic area, to our knowledge. Consistently, Ti remains the least soluble element and we can suppose that other elements and of importance in biogeochemical cycles, such as Co, Ni and Cu, have solubilities at least equal to the solubility value of Ti (median $\pm\,\sigma = 63\,\% \pm 23\,\%$). Heimburger et al. (2013) reported an iron deposition flux of $33 \pm 1\,\mu g\,m^{-2}\,d^{-1}$ on the Kerguelen Islands. Applying the median ($\pm\,\sigma$) iron solubility of $82\,\% \pm 18\,\%$ (Table 4a), the deduced soluble iron flux is equal to $27 \pm 6\,\mu g\,m^2\,d^{-1}$ for this oceanic area. This value is three times higher than the dissolved iron flux in the Southern Indian Ocean according to the model proposed by Fan et al. (2006) taking into account solubility processes with a 17 % average solubility calculated for modelled wet deposition, the predominant atmospheric deposition type on the

Kerguelen Islands (Heimburger et al., 2012a). To conclude, this experiment produced results for five validated samples only, but strongly suggests that solubility processes should be re-evaluated, as should soluble depositions simulated by current atmospheric models for remote oceanic areas such as the Southern Ocean.

Supplementary material related to this article is available online at http://www.biogeosciences.net/10/6617/2013/bg-10-6617-2013-supplement.pdf.

The publication of this article is financed by CNRS-INSU.

References

Annett, A. L., Lapi, S., Ruth, T. J., and Maldonado, M. T.: The effects of Cu and Fe availability on the growth and Cu:C ratios of marine diatoms, Limnol. Oceanogr., 53, 2451–2461, doi:10.4319/lo.2008.53.6.2451, 2008.

Baker, A. R. and Croot, P. L.: Atmospheric and marine controls on aerosol iron solubility in seawater, Mar. Chem., 120, 4–13, doi:10.1016/j.marchem.2008.09.003, 2010.

Baker, A. R. and Jickells, T. D.: Mineral particle size as a control on aerosol iron solubility, Geophys. Res. Lett., 33, L17608, doi:10.1029/2006GL026557, 2006.

Baker, A. R., Jickells, T. D., Witt, M., and Linge, K. L.: Trend in the solubility of iron, aluminium, manganese and phosphorus in aerosol collected over the Atlantic Ocean, Mar. Chem., 98, 43–58, doi:10.1016/j.marchem.2005.06.004, 2006.

Bhattachan, A., D'Odorico, P. , Baddock, M. C., Zobeck, T. M., Okin, G. S., and Cassar, N.: The Southern Kalahari: a potential new dust source in the Southern Hemisphere?, Environ. Res. Lett., 7, 7 pp., doi:10.1088/1748-9326/7/2/024001, 2012.

Blain, S., Quéguiner, B., Armand, L., Belviso, S., Bombled, B., Bopp, L., Bowie, A., Brunet, C., Brussard, C., Carlotti, F., Christaki, U., Corbière, A., Durand, I., Ebersbach, F., Fuda, J-L., Garcia, N., Gerringa, L., Griffiths, B., Guigue, C., Guillerm, C., Jacquet, S., Jeandel, C., Laan, P., Lefèvre, D., Monaco, C. L.,

Malits, A., Mosseri, J., Obernosterer, I., Park, Y.-H., Picheral, M., Pondaven, P., Remenyi, T., Sandroni, V., Sarthou, G., Savoye, N., Scouarnec, L., Souhaut, M., Thuiller, D., Timmermans, K., Trull, T., Uitz, J., van Beek, P., Veldhuis, M., Vincent, D., Viollier, E., Vong, L., T., and Wagener, T.: Effect of natural iron fertilization on carbon sequestration in the Southern Ocean, Nature, 446, 1070–1074, doi:10.1038/nature05700, 2007.

Boyd, P. W.: Environnemental factors controlling phytoplankton processes in the Southern Ocean, J. Phycol., 38, 844–861, 2002.

Boyd, P. W., Watson, A. J., Law, C. S., Abraham, E. R., Trull, T., Murdoch, R., Bakker, D. C., Bowie, A. R., Buesseler, K. O., Chang, H., Charette, M., Croot, P., Downing, K., Frew, R., Gall, M., Hadfield, M., Hall, J., Harvey, M., Jameson, G., LaRoche, J., Liddicoat, M., Ling, R., Maldonado, M., McKay, R. M., Nodder, S., Pickmere, S., Pridmore, R., Rintoul, S., Safi, K., Sutton, P., Strzepek, R., Tanneberger, K., Turner, S.,Waite, A., and Zeldis, J.: A mesoscale phytoplankton bloom in the polar Southern Ocean stimulated by iron fertilization, Nature, 407, 695–702, doi:10.1038/35037500, 2000.

Boyd, P. W., Jickells, T. D., Law, C. S., Blain, S., Boyle, E. A., Buesseler, K. O., Coale, K. H., Cullen, J. J., de Baar, H. J. W., Follows, M., Harvey, M., Lancelot, C., Levasseur, M., Owens, N. P. J., Pollard, R., Rivkin, R. B., Sarmiento, J., Schoemann, V., Smetacek, V., Takeda, S., Tsuda, A., Turner, S., and Watson, A. J.: Mesoscale Iron Enrichment Experiments 1993–2005: Synthesis and Future Directions, Science, 315, 612–617, doi:10.1126/science.1131669, 2007.

Boyd, P. W., Mackie, D. S., and Hunter, K. A.: Aerosol iron deposition to the surface ocean – Modes of iron supply and biological responses, Mar. Chem., 120, 128–143, doi:10.1016/j.marchem.2009.01.008, 2010.

Buck, S. C. and Paytan, A.: Evaluation of commonly used filtr substrates fro the measuremen of aerosol trace element solubility, Limnol. Oceanogr.-Meth., 10, 790–806, doi:10.4319/lom.2012.10.790, 2012.

Buck, S. C., Landing, W. M., and Resing, J. A.: Particle size and aerosol iron solubility: A high-resolution analysis of Atlantic aerosols, Mar. Chem., 120, 14–24, doi:10.1016/j.marchem.2008.11.002, 2010a.

Buck, C. S., Landing, W. M., Resing, J. A., and Measures, C. I.: The solubility and deposition of aerosol Fe and other trace elements in the North Atlantic Ocean: Observations from the A16N CLIVAR/CO2 repeat hydrography section, Mar. Chem., 120, 57–70, doi:10.1016/j.marchem.2008.08.003, 2010b.

Caldeira, K. and Duffy, P. B.: The role of the Southern Ocean in uptake and storage of anthropogenic carbon dioxide, Science, 287, 620–622, doi:10.1126/science.287.5453.620, 2000.

Chen, Y. and Siefert, R. L.: Seasonal and spatial distributions and dry deposition fluxes of atmospheric total and labil iron over the tropical and subtropical North Atlantic Ocean, J. Geophys. Res., 109, D09305, doi:10.1029/2003JD003958, 2004.

Colin, J.-L., Jaffrezo, J.-L., and Gros, J. M.: Solubility of major species in precipitation: factors of variation, Atmos. Environ., 24A, 537–544, doi:10.1016/0960-1686(90)90008-B, 1990.

de Baar, H. J. W., de Jong, J. T. M., Bakker, D. C. E., Loscher, B. M., Veth, C., Bathmann, U., and Smetacek, V.: Importance of iron for plankton blooms and carbon dioxide drawdown in the Southern Ocean, Nature, 373, 412–415, doi:10.1038/373412a0, 1995.

Desboeufs, K. V., Losno, R., and Colin, J.-L.: Factors influencing aerosol solubility during cloud processes, Atmos. Environ., 35, 3529–3537, doi:10.1016/S1352-2310(00)00472-6, 2001.

Desboeufs, K. V., Sofikitis, A., Losno, R., Colin, J.L., and Ausset, P.: Dissolution and solubility of race metals from natural and anthropogenic aerosol particulate matter, Chemosphere, 58, 195–203, doi:10.1016/j.chemosphere.2004.02.025, 2005.

Draxler, R. R. and Rolph, G. D.: HYSPLIT (HYbrid Single-Particle Lagrangian Integrated Trajectory) Model access via NOAA ARL READY Website (http://ready.arl.noaa.gov/HYSPLIT.php), NOAA Air Resources Laboratory, Silver Spring, MD, 2012.

Duce, R. and Tindale, N. W.: Chemistry and biology of iron and other trace metals, Limnol. Oceanogr., 36, 1715–1726, 1991.

Edwards, R. and Sedwick, P.: Iron in East Antarctic snow: Implications for atmospheric iron deposition and algal production in Antarctic waters, Geophys. Res. Lett., 28, 3907–3910, doi:10.1029/2001GL012867, 2001.

Feinberg, M.: Labo-stat – Guide de validation des méthodes d'analyse, Lavoisier, 361 pp., 2009.

Fan, S.-M., Moxim, W. J., and H. Levy II, H.: Aeolian input of bioavailable iron to the ocean, Geophys. Res. Lett., 33, L07602, doi:10.1029/2005GL024852, 2006.

Fung, I. Y., Meyn, S. K., Tegen, I., Doney, S. C., John, J. G., and Bishop, J. K. B.: Iron supply and demand in the upper ocean, Global Biogeochem. Cy., 14, 281–295, 2000.

Gieray, R., Wieser, P., Engelhardt., T., Swietlicki, E., Hansson, H. C., Mentes, B., Orsini, D., Martinsson, B., Svenningsson, B., Noone, K. J., and Heintzenberg, J.: Phase partitioning of aerosol constituents in cloud based on single-particle and bulk analysis, Atmos. Environ., 31, 2491–2502, 1997.

Guieu, C., Chester, R., Nimmo, M., Martin, J.-M., Guerzoni, S., Nicolas, E., Mateu J., and Keyse, S.: Atmospheric input of dissolved and particulate metals to the northwester Medierranean, Deep-Sea Res. II, 44, 655–674, doi:10.1016/S0967-0645(97)88508-6, 1997.

Hand, J.L., Mahowald, N. M., Chen, Y., Siefert, R.L., Luo, C., Bubrananiam, A., and Fung, I.: Estimates of atmosphérique-processed soluble iron from observations and a global mineral aerosol model: Biogeochemical implications, J. Geophys. Res., 109, D17205, doi:10.1029/2004JD004575, 2004.

Heimburger, A., Losno, R., Triquet, S., Dulac F., and Mahowald, N. M.: Direct measurements of atmospheric iron, cobalt and aluminium-derived dust deposition at Kerguelen Islands, Global Biogeochem. Cy., 26, GB4016, doi:10.1029/2012GB004301, 2012a.

Heimburger, A., Tharaud, M., Monna, F., Losno, R., Desboeufs, K., and Bon Nguyen, E.: SLRS-5 Elemental Concentrations of Thirty-Three Uncertified Elements Deduced from SLRS-5/SLRS-4 Ratios, Geostand. Geoanal. Res., 37, 77–85, doi:10.1111/j.1751-908X.2012.00185.x, 2012b.

Heimburger, A., Losno, R., Triquet, S., and Bon Nguyen, E.: Atmospheric deposition fluxes of 26 elements over the Southern Indian Ocean : Times series on Kerguelen and Crozet Islands, Global Biogeochem. Cy., 27, 440–449, doi:10.1002:gbc.20043, 2013.

Hsu, S.-C., Wong, G. T. F., Gong, G.-C., Shiah, F.-K., Huang, Y.-T., Kao, S.-J., Tsai, F., Lung, S.-C. C., Lin, F.-J., Lin, I.-I., Hung, C.-C., and Tseng, C.-M.: Sources, solubility, and dry deposition of aerosol trace elements over the East China Sea, Mar. Chem., 120, 116–127, doi:10.1016/j.marchem.2008.10.003, 2010.

Ito, A.: Contrasting the Effect of Iron Mobilization on Soluble Iron Deposition to the Ocean in the Northern and Southern Hemispheres, J. Meteorol. Soc. Japan, 90A, 167–188, doi:10.2151/jmsj.2012-A09, 2012.

Jickells, T. D., Davies, T. D., Tranter, M., Landsberger, S., Jarvis, K., and Abrahams, P.: Trace elements in snow samples from Scottish Higlands: sources and dissolved/particulate distributions, Atmos. Environ., 26A, 393–401, doi:10.1016/0960-1686(92)90325-F, 1992.

Jickells, T. D., An, Z. S., Andersen, K. K., Baker, A. R., Bergametti, G., Brooks, N., Cao, J. J., Boyd, P. W., Duce, R. A., Hunter, K. A., Kawahata, H., Kubilay, N., LaRoche, J., Liss, P. S., Mahowald, N., Prospero, J. M., Ridgwell, A. J., Tegen, I., and Torres, R.: Global Iron Connections Between Desert Dust, Ocean Biogeochemistry, and Climate, Science, 308, 67–71, doi:10.1126/science.1105959, 2005.

Journet, E., Desboeufs, K. V., Caquineau, S., and Colin, J.-L.: Mineralogy as a critical factor of dust iron solubility, Geophys. Res. Lett, 35, L07805, doi:10/1029/2007/GL031589, 2008.

Kieber, R. J., Willey, J. D., and Avery Jr., G. B.: Temporal variability of rainwater iron speciation at the Bermuda Atlantic Time Series Station, J. Geophys. Res., 108, C83277, doi:10.1029/2001JC001031, 2003.

Lim, B., Jickells, T. D., Colin, J.-L., and Losno, R.: Solubilities of Al, Pb, Cu, and Zn in rain sampled in the marine environment over the North Atlantic Ocean and Mediterranean Sea, Global Biogeochem. Cy., 8, 349–362, doi:10.1029/94GB01267, 1994.

Losno, R.: Chimie d'éléments minéraux en trace dans les pluies méditerranéennes, Ph.D. Thesis, Université de Paris 7, 1989.

Losno, R., Colin, J.-L., Lebris, N., Bergametti, G., Jickells, T., and Lim, B.: Aluminium solubility in rainwater and molten snow, J. Atmos. Chem., 17, 29–43, doi:10.1007/BF00699112, 1993.

Mahowald, N. M.: Anthropocene changes in desert area: Sensitivity to climate model predictions, Geophys. Res. Lett., 34, L18817, doi:10.1029/2007GL030472, 2007.

Mahowald, N. M., Baker, A. R., Bergametti, G., Brooks, N., Duce, R. A., Jickells, T. D., Kubilay, N., Prospero, J. M., and Tegen, I.: Atmospheric global dust cycle and iron inputs to the ocean, Global Biogeochem. Cy., 19, GB4025, doi:10.1029/2004GB002402, 2005.

Martin, J. H.: The iron hypothesis, Paleoceanography, 5, 1–13, 1990.

Middag, R., de Baar, H. J. W., Laan, P., Cai, P. H., van Ooijen, J. C.: Dissolved manganese in the Atlantic sector of the Southern Ocean, Deep-Sea Res. II, 58, 2661–2677, doi:10.1016/j.drs2.2010.10.043, 2011.

Morel, F. M. M. and Price, N. M.: The Biogeochemical Cycles of Trace Metals in the Oceans, Science, 300, 944–948, doi:10.1126/science.1083545, 2003.

Morel, F. M., Hudson, R. J. M., and Price, N. M.: Limitation of productivity by trace metals in the sea, Limnol. Oceanogr., 36, 1742–1755, doi:10.4319/lo.1991.36.8.1742, 1991.

Morton, P.L., Landing W. M., Hsu S.-C., Milne A., Aguilar-Islas A. M. , Baker A. R., Bowie A. R., Buck C. S., Gao Y., Gichuki S., Hastings G. M., Hatta M., Johansen A. M., Losno R., Mead C., Patey M. D., Swarr G., Vandermark A., and Zamora L. M: Methods for the sampling and analysis of ma-

rine aerosols: results from the 2008 GEOTRACES aerosol intercalibration experiment, Limnol. Oceanogr.-Meth., 11, 62–78, doi:10.4319/lom.2013.11.62, 2013.

Paris, R., Desboeufs, K. V., Formenti, P., Nava, S., and Chou, C.: Chemical characterisation of iron in dust and biomass burning aerosols during AMMA-SOP0/DABEX: implication for iron solubility, Atmos. Chem. Phys., 10, 4273–4282, doi:10.5194/acp-10-4273-2010, 2010.

Paris, R., Desboeufs, K. V., and Journet, E.: Variability of dust iron solubility in atmospheric waters: investigation of the role of oxalate organic complexation, Atmos. Chemi. Phys., 45, 5510–5517, doi:10.1016/j.atmosenv.2011.08.068, 2011.

Price, N. M. and Morel, F. M. M.: Colimitation of phytoplankton growth by nickel and nitrogen, Limnol. Oceanogr., 36, 1071–1077, doi:10.4319/lo.1991.36.6.1071, 1991.

Prospero, J. M., Ginoux, P., Torres, O., Nicholson, S. E., and Gill, T. E.: Environmental characterization of global sources of atmospheric soil dust identified with the NIMBUS 7 TOMS absorbing aerosol product, Rev. Geophys., 40, 2-1–2-31, 2002.

Pruppacher, H. R. and Jaenicke, R.: Processing of water-vapor and aerosols by atmospheric clouds, a global estimate, Atmos. Res., 38, 283–295, doi:10.1016/0169-8095(94)00098-X, 1995.

Rolph, G. D.: Real-time Environmental Applications and Display sYstem (READY) Website (http://ready.arl.noaa.gov), NOAA Air Resources Laboratory, Silver Spring, MD, 2012.

Saito, M. A., Moffett, J. W., Chisholm, S. W., and Waterbury, J. B.: Cobalt limitation and uptake in Prochlorococcus, Limnol. Oceanogr., 47, 1629–1636, doi10.4319/lo.2002.47.6.1629, 2002.

Sarmiento, J. L., Hughes, T. M. C., Stouffer, R. J., and Manabe, S.: Simulated response of the ocean carbon cycle to anthropogenic climate warming, Nature, 393, 245–249, doi:10.1038/30455, 1998.

Schlitzer, R.: Applying Adjoint Method for Biogeochemical Modeling: Export of Particulate Organic Matter in the World Ocean, Geoph. Monog. Ser., 114, 107–124, 2000.

Shi, Z., Krom, M. D., Jickells, T. D., Bonneville, S., Carslaw, K. S., Mihalopoulos, N., Baker, A. R., and Benning, L. G.: Impacts on iron solubility in the mineral dust by processes in the source region and the atmosphere: A review, Aeolian Res., 5, 21–42, doi:10.1016/j.aeolia.2012.03.001, 2012.

Siefert, R. L., Johansen, A. M., and Hoffmann, M. R.: Chemical characterization of ambient aerosol collected during the southwest monsoon and inter-monsoon seasons over the Arabian Sea: Labile-Fe(II) and other trace metals, J. Geophys. Res., 104, 3511–3526, doi:10.1029/1998JD100067, 1999.

Theodosi, C., Markaki, Z., Tselepides, A., and Mihalopoulos, N.: The significance of atmospheric inputs of soluble and particulate major and trace metals to the eastern Mediterranean seawater, Mar. Chem., 120, 154–163, doi:10.1016/j.marchem.2010.02.003, 2010.

Visser, F., Gerringa, L. J. A., Van der gaast, S. J., de Baar, H. J. W., and Timmermans, K. R.: The role of the reactivity and content of iron of aerosol dust on growth rates of two antarctic diatom species, J. Phycol, 39, 1085-1094, doi:10.1111/j.0022-3646.2003.03-023.x, 2003.

Wagener, T., Guieu, C., Losno, R., Bonnet, S., and Mahowald, N.: Revisiting atmospheric dust export to the Southern Hetmisphere ocean: Biogeochemical implications, Global Biogeochem. Cy., 22, GB2006, doi:10.1029/2007GB002984, 2008.

Witt, M.L.I., Mather, T. A., Baker, A. R., De Hoog, J. C. M., and Pyle, D.M.: Atmospheric trace metals over the south-west Indian Ocean: Total gaseous mercury, aerosol trace metal concentrations and lead isotope ratios, Mar. Chem., 121, 2–16, doi:10.1016/j.marchem.2010.02.005, 2010.

Zhuang, G.,. Yi, Z., Duce, R. A., and Brown, P. R. : Chemistry of iron in Marine aerosols, Global Biogeochem. Cy., 6, 161–173, doi:10.1029/92GB00756, 1992.